Title

Formation of Hexacoordinate Mn(III) in Bacillus subtilis Oxalate Decarboxylase Requires Catalytic Turnover

Journal

Biochemistry, 55(3)

ISSN

0006-2960

Authors

Zhu, Wen
Wilcoxen, Jarett
Britt, R David
et al.

Publication Date

2016-01-26

DOI

10.1021/acs.biochem.5b01340

Peer reviewed

HHS Public Access

Author manuscript

Biochemistry. Author manuscript; available in PMC 2021 June 07.

Published in final edited form as:

Biochemistry. 2016 January 26; 55(3): 429–434. doi:10.1021/acs.biochem.5b01340.

Formation of Hexacoordinate Mn(III) in *Bacillus subtilis* Oxalate Decarboxylase Requires Catalytic Turnover

Wen Zhu[#†], **Jarett Wilcoxen**[#‡], **R. David Britt**[*,‡], **Nigel G. J. Richards**[*,†,§]

[†]Department of Chemistry & Chemical Biology, Indiana University Purdue University Indianapolis, Indianapolis, Indiana 46202, United States

[‡]Department of Chemistry, University of California, Davis, California 95616, United States

[#] These authors contributed equally to this work.

Abstract

Oxalate decarboxylase (OxDC) catalyzes the disproportionation of oxalic acid monoanion into CO_2 and formate. The enzyme has long been hypothesized to utilize dioxygen to form mononuclear Mn(III) or Mn(IV) in the catalytic site during turnover. Recombinant OxDC, however, contains only tightly bound Mn(II), and direct spectroscopic detection of the metal in higher oxidation states under optimal catalytic conditions (pH 4.2) has not yet been reported. Using parallel mode electron paramagnetic resonance spectroscopy, we now show that substantial amounts of Mn(III) are indeed formed in OxDC, but only in the presence of oxalate and dioxygen under acidic conditions. These observations provide the first direct support for proposals in which Mn(III) removes an electron from the substrate to yield a radical intermediate in which the barrier to C−C bond cleavage is significantly decreased. Thus, OxDC joins a small list of enzymes capable of stabilizing and controlling the reactivity of the powerful oxidizing species Mn(III).

Graphical Abstract

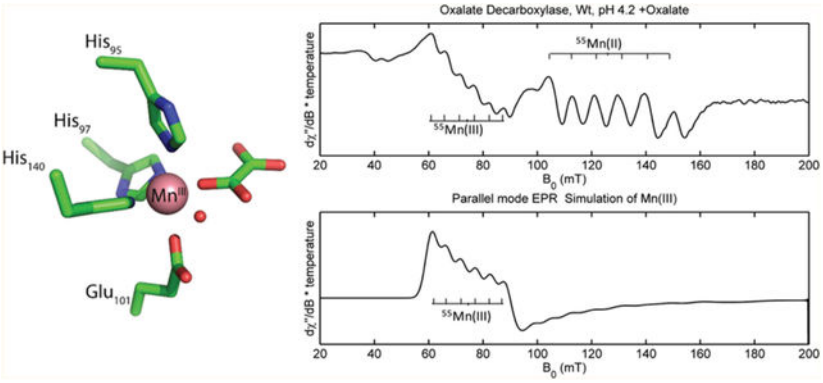

[*]**Corresponding Authors:** rdbritt@ucdavis.edu. richardsN14@cardiff.ac.uk.

[§]**Present Address**: N.G.J.R.: School of Chemistry, Cardiff University, Park Place, Cardiff CF10 3AT, U.K.

The authors declare no competing financial interest.

Supporting Information

The Supporting Information is available free of charge on the ACS Publications website at DOI: 10.1021/acs.biochem.5b01340.

Supplemental Figures S1–S4 and Tables S1 and S2 (PDF)

Manganese-dependent enzymes process spectacular chemical transformations,[1–3] by manipulating the redox properties of the metal, predominantly using multimetal centers. Less is known, however, about how proteins modulate the reactivity of mononuclear manganese sites in which the metal is tightly bound.[4,5] Oxalate decarboxylase (OxDC) catalyzes the cleavage of the C−C bond in oxalate under acidic conditions to give formate and CO_2 (Scheme 1)[6,7] and is of general interest because, somewhat unusually, catalytic activity requires manganese and dioxygen even though the reaction is formally a disproportionation.[8–11] Moreover, reactions that break the C−C bond between two sp^2-hybridized atoms without the use of cofactors, such as thiamine diphosphate, are rare in biochemistry.[12,13] Heavy-atom isotope effect measurements[8] and spin-trapping experiments[11,14] suggest that C−C bond cleavage takes place in a radical intermediate that is formed by removal of an electron from the substrate, in what has been proposed to be a proton-coupled electron transfer (PCET) reaction (Scheme 1).[10] Calculations show that the barrier to decarboxylation in oxalate-based radicals is lowered by up to 30 kcal/mol,[15] providing support for the involvement of radical intermediates in the catalytic mechanism. We,[8] and others,[16] have speculated that the role of dioxygen is to oxidize the catalytically important Mn(II) ion into a higher oxidation state, such as Mn(III), which can then oxidize the bound substrate to the appropriate radical intermediate (Scheme 1). The mismatched reduction potentials of dioxygen and Mn(III), and a dearth of model Mn-containing inorganic complexes capable of binding and activating dioxygen,[17–19] provide evidence against such a proposal. Indeed, the direct spectroscopic detection of bound mononuclear Mn(III) or Mn(IV) ions in OxDC under optimal catalytic conditions (pH 4.2) has not been reported. In part, this reflects the fact that only one of the two bound manganese ions (located in the N-terminal domain) likely mediates catalysis,[20–23] which has greatly complicated any spectroscopic characterization of the enzyme using EPR methods (Figure S1 of the Supporting Information).[24–27] Although prior EPR studies did find weak evidence of the presence of Mn(III),[27] any clear mechanistic interpretation of that data is complicated by the presence of Mn(III) in the C-terminal site of wild-type (wt) OxDC at high pH.[20,24] We now report parallel mode EPR measurements that unambiguously demonstrate Mn(III) formation in wt OxDC under V_{max} conditions (100 mM oxalate at pH 4.2), which have been made possible by the development of new methods for obtaining high concentrations (0.5 mM) of the pure enzyme.

EXPERIMENTAL PROCEDURES

Expression and Purification of Recombinant, wt OxDC Samples Used in This Study.

Recombinant, His_6-tagged wt OxDC was expressed and purified following published procedures[6] with minor modifications to avoid protein precipitation during concentration. Thus, expression was induced in the presence of 5 mM $MnCl_2$ after heat shocking the bacteria for 15 min at 42 °C with constant agitation. After the addition of IPTG, cultures were incubated at 37 °C for 5 h before being harvested by centrifugation at 2000*g* for 20 min (4 °C) and sonicated in lysis buffer. The resulting supernatant was centrifuged at 20000*g* for 20 min (4 °C) before the enzyme was purified from the cleared lysate by metal affinity chromatography on a Ni-NTA column. The eluted protein was subjected to dialysis at 4 °C to give a solution in 50 mM Tris buffer containing 20% glycerol and 500 mM NaCl (pH

8.5). Storage buffers also contained 20% glycerol. Protein concentrations were determined using the CoomassiePlus Protein Assay reagent obtained from ThermoFisher Scientific (Waltham, MA), and the metal content of purified, recombinant wt OxDC (Table S1) was obtained at the University of Georgia Center for Applied Isotope Studies Chemical Analysis Laboratory (Athens, GA).

Kinetic Characterization of Recombinant, wt OxDC Samples Used in This Study.

To confirm that recombinant, His_6-tagged wt OxDC was active, steady-state kinetic parameters were measured using membrane inlet mass spectrometry (MIMS) for [$^{13}C_2$]oxalate in 50 mM potassium acetate buffer (pH 4.2), as described previously.[28,29] $13CO_2$ production (Figure S2) was monitored by measuring the m/z 45 ion current and converted to millimolar concentration using a standard curve. Measurements were taken at specific substrate and enzyme concentrations in triplicate, and the data were analyzed to obtain the values of V and V/K by standard computer-based methods.[30] Formate production was confirmed using an end-point assay, as described elsewhere.[8] The V_{max} (22 ± 3 units/mg) was redetermined for the highly concentrated enzyme solutions used in the EPR measurements that also contained glycerol. Thus, reaction was initiated by adding wt OxDC (44 mg/mL) to poly buffer (100 mM sodium citrate, 50 mM Bis-Tris, and 25 mM Tris-HCl containing 30% glycerol) containing 200 mM oxalate. After 15 s, the reaction was quenched by the addition of aqueous NaOH and the amount of formate determined.

EPR Characterization of Recombinant, wt OxDC Samples Used in This Study.

Samples used for EPR analysis were incubated with Chelex resin for 2 h on ice to remove free metal ions from the buffer before being concentrated to approximately 27 mg/mL using an Amicon Centriprep YM-30 filter unit from Millipore (Billerica, MA). EPR measurements of the enzyme samples were performed in poly buffer (100 mM sodium citrate, 50 mM Bis-Tris, and 25 mM Tris-HCl containing 30% glycerol) in samples adjusted to pH 8.5, 5.7, and 4.2. For oxalate-containing samples, 200 mM potassium oxalate was added at each solution pH (final concentration of 100 mM), and the resulting solutions were mixed in the EPR tube at room temperature to initiate the reaction. After 15 s, each sample was flash-frozen in an acetone/dry ice slush and stored in liquid N_2. The final protein concentrations for each experimental EPR measurement are listed in Table S2. An extended reaction sample was prepared using an identical procedure except that the reaction time was extended to 5 min. The rapid-freeze quench reaction was performed by mixing a protein solution containing 50% glycerol and oxalate in pH 4.2 poly buffer for 10 ms before the mixture was rapidly frozen to quench the reaction. In this freeze quench experiment, the final concentrations of enzyme and oxalate were 500 ± 70 μM and 100 mM, respectively. On the basis of the independent determination of V_{max} under these conditions (see above), the estimated level of formate produced after 10 ms is 8 μM.

Samples for X-band (~9.4 GHz) EPR spectroscopy were measured at the CalEPR center (University of California, Davis, CA). Continuous wave (CW) spectra were recorded using a Brüker Instruments EleXsys-II E500 CW EPR spectrometer (Bruker, Billerica, MA) equipped with an Oxford Instruments ESR900 liquid helium cryostat and Oxford Instruments ITC503 temperature and gas-flow controller. Samples were measured under

nonsaturating slow-passage conditions using a Super-High Q resonator (ER 4122SHQE) or Dual Mode resonator (ER 4116DM); specific parameters for microwave frequencies, modulation amplitude, and temperature are included in the figure legends.

RESULTS AND DISCUSSION

Recombinant wt *Bacillus subtilis* OxDC containing 1.5 Mn(II) ions/monomer was obtained by expression in *Escherichia coli* following standard protocols (see the Supporting Information). The enzyme was dissolved in poly buffer (100 mM sodium citrate, 50 mM Bis-Tris, and 25 mM Tris-HCl containing 500 mM KCl) containing 30% glycerol at concentrations ranging from 460 to 590 μM. Under these conditions, decarboxylase activity at pH 4.2 was determined by measuring CO_2 production using membrane inlet mass spectrometry (Figure S2 of the Supporting Information).[27,28] Perpendicular and parallel mode X-band EPR spectra of wt OxDC protein were recorded at pH 8.5, 5.7, and 4.2 to characterize the properties of the manganese centers in the enzyme (Figure 1). At pH 8.5, OxDC does not catalyze substrate decarboxylation because only the monoprotonated form of oxalate is the true substrate.[8] In agreement with previous EPR observations,[24] the sample exhibited a characteristic signal for the hyperfine-split transition of Mn(II) at $g = 2.0$ in perpendicular mode EPR together with a sextet feature near $g_{eff} = 4.3$ that can be attributed to the half-field transition (Figure 1A). The parallel mode EPR spectrum of wt OxDC at pH 8.5 exhibited a distinctive sextet signal, corresponding to the $\Delta m_s = \pm 2$ transition of Mn(II), but no Mn(III) signal was present under these conditions (Figure 1B), confirming the findings of other EPR studies.[24–27] In contrast, the presence of oxalate at pH 5.7 and 4.2, where wt OxDC exhibits catalytic activity, caused substantial changes in both the perpendicular and parallel mode EPR spectra (Figure 1C,D). Most importantly, a new sextet signal centered near 75 mT appears in the parallel mode spectrum at pH 4.2 and 5.7 (Figure 1D), which was hypothesized to be associated with enzyme-bound Mn(III). The gradual disappearance of this signal with an increasing solution pH suggests that the presence of this species is likely correlated with the catalytic activity of the enzyme.[8] Simulations to confirm the nature of the Mn species present in wt OxDC when oxalate was present were performed with the EasySpin tool box (version 4.5.5) in Matlab (Mathworks Inc., Natick, MA).[31] The pH dependence of the high-field EPR (HFEPR) spectra for wt OxDC in the absence of oxalate over a pH range of 4.0–8.8 has been reported,[24] revealing six unique EPR spectra associated with two Mn coordination sites in the enzyme, with distinct transitions related to ligand protonation events. Site 1, where catalysis takes place, has two unique spectra, and site 2, the auxiliary site, has four unique spectra. In agreement with these prior observations, we find that wt OxDC has a similar mix of species present in perpendicular mode EPR spectra at equilibrium regardless of whether oxalate is present (Figure 1).

In simulations of the parallel mode spectra, we approximated the Mn(II) species using parameters given in the earlier work and were able to reproduce the signal arising from the forbidden transition of the Mn(II) species seen in the parallel mode EPR spectra (Figure 2). The hyperfine features that arise from the ^{55} Mn ($I = {}^5/_2$) signal assigned to the enzyme-bound Mn(III) – oxalate complex and resting Mn(II) are well reproduced using very different values of 150 and 253 MHz for the hyperfine coupling of the Mn(III) and Mn(II) species, respectively. To determine the sign of the zero-field splitting (ZFS) for the $S = 2$

species observed via parallel mode EPR, we measured the temperature dependence of the spectrum (Figure S3 of the Supporting Information). The Curie law behavior of the spectrum reveals a negative value for the ZFS, with the following simulation parameters: $D = -120$ GHz, and $|E| = 13.2$ GHz, where D is the axial ZFS parameter and E is the rhombic ZFS parameter. These values are similar to those used to model compounds containing a mix of oxygen and nitrogen ligands similar to the environment of the two Mn ions in wt OxDC (Scheme 1).[32] The negative ZFS value and magnitude of the hyperfine splitting indicates a $^5B_1$ symmetry ground state for either a six-coordinate or five-coordinate square pyramidal Mn(III).[33] Given that there is no structural or spectroscopic evidence of the latter coordination,[16,20−22,24−27] it seems likely that oxalate binding results in the formation of a six-coordinate Mn(III) species. To the best of our knowledge, this is the first unambiguous demonstration that one of the metal centers is oxidized to Mn(III) in the presence of oxalate and dioxygen under acidic conditions. Moreover, and in contrast to previous claims,[20] the parallel mode EPR spectrum of wt OxDC in the absence of substrate over the pH range of 4.2–8.5 provides no evidence of the existence of Mn(III) in the "as-purified" enzyme from *E. coli*.

To confirm the Mn(III) signal is observed during the catalytic cycle of OxDC, the spectrum of an OxDC/oxalate sample, at pH 4.2, in which almost all the substrate had been consumed, was measured by parallel mode EPR. The "forbidden" transition of Mn(II) was observed together with a small Mn(III) sextet, which was decreased at least 20-fold compared to those of identical samples undergoing turnover (Figure S4 of the Supporting Information). Any lingering Mn(III) may arise from rebinding formate in the presence of oxygen, although the K_i value for formate is >200 mM. Residual Mn(III) in the sample may also reflect a small amount of enzyme undergoing reaction during the measurement. Reduction of the magnitude of the Mn(III) signal with oxalate consumption also supports the view that Mn(III) formation requires OxDC-mediated catalysis. When oxalate has been consumed, OxDC-bound Mn(III) is cycled back to Mn(II), perhaps with oxidation of a proximal tyrosine residue.[27] Similarly, in parallel mode EPR spectra of samples subject to rapid freeze quench (<15 ms) (Figure S5 of the Supporting Information), there was no observable Mn(III) signal, suggesting that Mn(III) forms after oxalate becomes bound prior to turnover. We also note that the presence of high glycerol concentrations required for this experiment slows the reaction rate by approximately 2-fold.

These parallel mode EPR observations provide the first evidence of higher Mn oxidation states during OxDC-catalyzed oxalate breakdown. The identification of conditions for observing OxDC-bound Mn(III) by parallel mode EPR will also permit a systematic investigation of how protein residues might control metal reactivity. Questions remain, however, concerning (i) which of the two Mn(II) centers is oxidized and (ii) the mechanism by which dioxygen becomes able to oxidize OxDC-bound Mn(II) to Mn(III). We suggest that the Mn(III) signal is associated with the metal center in the N-terminal domain of the enzyme. An earlier pH-dependent HFEPR study of wt OxDC showed that the signal from the N-terminal metal-binding site is more sensitive to changes in buffer pH,[25] presumably because it is more accessible to solvent[23] due to the presence of a mobile loop that can exist in open and closed conformations.[22] Of course, given that 100 mM oxalate is needed to observe Mn(III), we cannot rule out the possibility that substrate does not access the C-

terminal Mn-binding site. With both the requirement of dioxygen for catalytic activity[7,34] and the finding that superoxide radicals are formed under turnover conditions,[14] it seems reasonable to propose that dioxygen mediates metal oxidation (Scheme 1). A previous parallel mode EPR study of a synthetic monomeric Mn complex, which exhibits spectroscopic properties similar to those exhibited by OxDC, has suggested that formation of the superoxo–Mn(III) complex precedes production of the hydroperoxo–Mn(III) complex.[35] The fact that oxalate is required for the formation of Mn(III) is therefore chemically intriguing given that protein environments can modulate the redox potential of Mn(II).[4] Precedent for the idea that oxalate binding is needed for Mn(III) formation is provided by a Mn-dependent dioxygenase present in *Arthrobacter globiformis*, which binds a deprotonated catechol substrate prior to dioxygen activation.[36] In addition, studies of the interaction of the Mn centers in OxDC with nitric oxide (NO) as a dioxygen mimic suggest that NO does not bind to the Mn(II) centers in the free enzyme.[29] We suggest that oxalate binding is required before dioxygen is able to coordinate the active site metal and give rise to Mn(III). The Mn(III)–superoxide "system" could then function as an electron sink to form the Mn-bound oxalate radical needed to lower the barrier to heterolytic cleavage of the C−C bond.[15] Unlike redox Mn enzymes that adapt multinuclear metal center and process redox catalysis,[1] the redox cycle in OxDC is, to the best of our knowledge, the first example of a hexacoordinate, mononuclear, manganese-dependent enzyme capable of mediating the interconversion of Mn(II) and Mn(III) using dioxygen as a "cofactor". Exactly how OxDC stabilizes and controls the reactivity of Mn(III), which is a powerful oxidant in aqueous solution, remains to be determined.

Supplementary Material

Refer to Web version on PubMed Central for supplementary material.

ACKNOWLEDGMENTS

A plasmid encoding the C-terminally His_6-tagged wt OxDC was generously provided by Dr. Stephen Bornemann (John Innes Centre, Norwich, U.K.).

Funding

These studies were funded by the National Institutes of Health (Grant DK-061666 to N.G.J.R. and Grant GM-104543 to R.D.B.).

ABBREVIATIONS

OxDC	oxalate decarboxylase
PCET	proton-coupled electron transfer
wt	wild type
MIMS	membrane inlet mass spectrometry
NO	nitric oxide
ZFS	zero-field splitting

FDH	formate dehydrogenase

REFERENCES

(1). Nelson N, and Junge W (2015) Structure and energy transfer in photosystems of oxygenic photosynthesis. Annu. Rev. Biochem 84, 659–683. [PubMed: 25747397]

(2). Whittaker JW (2012) Non-heme manganese catalase - The 'other' catalase. Arch. Biochem. Biophys 525, 111–120. [PubMed: 22198285]

(3). Cotruvo JA Jr., and Stubbe J (2011) *Escherichia coli* class Ib ribonucleotide reductase contains a dimanganese(III)-tyrosyl radical cofactor *in vivo*. Biochemistry 50, 1672–1681. [PubMed: 21250660]

(4). Miller A-F (2008) Redox tuning over almost 1 V in a structurally conserved active site: Lessons from Fe-containing superoxide dismutase. Acc. Chem. Res 41, 501–510. [PubMed: 18376853]

(5). Borgstahl GEO, Parge H, Hickey MJ, Beyer WF, Hallewell RA, and Tainer JA (1992) The structure of human mitochondrial manganese superoxide dismutase reveals a novel tetrameric interface of 2 4-helix bundles. Cell 71, 107–118. [PubMed: 1394426]

(6). Moomaw EW, Angerhofer A, Moussatche P, Ozarowski A, Garcia-Rubio I, and Richards NGJ (2009) Metal dependence of oxalate decarboxylase activity. Biochemistry 48, 6116–6125. [PubMed: 19473032]

(7). Tanner A, Bowater L, Fairhurst SA, and Bornemann S (2001) Oxalate decarboxylase requires manganese and dioxygen for activity. J. Biol. Chem 276, 43627–43634. [PubMed: 11546787]

(8). Reinhardt LA, Svedruzic D, Chang CH, Cleland WW, and Richards NGJ (2003) Heavy atom isotope effects on the reaction catalyzed by the oxalate decarboxylase from *Bacillus subtilis*. J. Am. Chem. Soc 125, 1244–1252. [PubMed: 12553826]

(9). Svedruzic D, Liu Y, Reinhardt LA, Wroclawska E, Cleland WW, and Richards NGJ (2007) Investigating the roles of putative active site residues in the oxalate decarboxylase from *Bacillus subtilis*. Arch. Biochem. Biophys 464, 36–47. [PubMed: 17459326]

(10). Saylor BT, Reinhardt LA, Lu Z, Shukla MS, Nguyen L, Cleland WW, Angerhofer A, Allen KN, and Richards NGJ (2012) A structural element that facilitates proton-coupled electron transfer in oxalate decarboxylase. Biochemistry 51, 2911–2920. [PubMed: 22404040]

(11). Imaram W, Saylor BT, Centonze C, Richards NGJ, and Angerhofer A (2011) EPR spin trapping of an oxalate-derived free radical in the oxalate decarboxylase reaction. Free Radical Biol. Med 50, 1009–1015. [PubMed: 21277974]

(12). Radzicka A, and Wolfenden R (1995) A proficient enzyme. Science 267, 90–93. [PubMed: 7809611]

(13). Becker A, Fritz-Wolf K, Kabsch W, Knappe J, Schultz S, and Volker Wagner AF (1999) Structure and mechanism of the glycyl radical enzyme pyruvate formate-lyase. Nat. Struct. Biol 6, 969–975. [PubMed: 10504733]

(14). Twahir UT, Stedwell CN, Lee CT, Richards NGJ, Polfer NC, and Angerhofer A (2015) Observation of superoxide production during catalysis of *Bacillus subtilis* oxalate decarboxylase at pH 4. Free Radical Biol. Med 80, 59–66. [PubMed: 25526893]

(15). Molt RW Jr., Lecher AM, Clark T, Bartlett RJ, and Richards NGJ (2015) Facile C_{sp2}-C_{sp2} bond cleavage in oxalic acid-derived radicals. J. Am. Chem. Soc 137, 3248–3252. [PubMed: 25702589]

(16). Anand R, Dorrestein PC, Kinsland C, Begley TP, and Ealick SE (2002) Structure of oxalate decarboxylase from *Bacillus subtilis* at 1.75 Å resolution. Biochemistry 41, 7659–7669. [PubMed: 12056897]

(17). Coggins MK, Sun X, Kwak Y, Solomon EI, Rybak-Akimova E, and Kovacs JA (2013) Characterization of metastable intermediates formed in the reaction between a Mn(II) complex and dioxygen, including a crystallographic structure of a binuclear Mn(III)-peroxo species. J. Am. Chem. Soc 135, 5631–5640. [PubMed: 23470101]

(18). Rees JA, Martin-Diaconescu V, Kovacs JA, and DeBeer S (2015) X-ray absorption and emission study of dioxygen activation by a small-molecule manganese complex. Inorg. Chem 54, 6410–6422. [PubMed: 26061165]

(19). Wijeratne GB, Corzine B, Day VW, and Jackson TA (2014) Saturation kinetics in phenolic O-H bond oxidation by a mononuclear Mn(III)-OH complex derived from dioxygen. Inorg. Chem 53, 7622–7634. [PubMed: 25010596]

(20). Burrell MR, Just VJ, Bowater L, Fairhurst SA, Requena L, Lawson DM, and Bornemann S (2007) Oxalate decarboxylase and oxalate oxidase activities can be interchanged with a specificity switch of up to 282,000 by mutating an active site lid. Biochemistry 46, 12327–12336. [PubMed: 17924657]

(21). Just VJ, Burrell MR, Bowater L, McRobbie I, Stevenson CE, Lawson DM, and Bornemann S (2007) The identity of the active site of oxalate decarboxylase and the importance of the stability of active-site lid conformations. Biochem. J 407, 397–406. [PubMed: 17680775]

(22). Just VJ, Stevenson CE, Bowater L, Tanner A, Lawson DM, and Bornemann S (2004) A closed conformation of *Bacillus subtilis* oxalate decarboxylase OxDc provides evidence for the true identity of the active site. J. Biol. Chem 279, 19867–19874. [PubMed: 14871895]

(23). Karmakar T, Periyasamy G, and Balasubramanian S (2013) CO_2 migration pathways in oxalate decarboxylase and clues about its active site. J. Phys. Chem. B 117, 12451–12460. [PubMed: 24053484]

(24). Tabares LC, Gätjens J, Hureau C, Burrell MR, Bowater L, Pecoraro VL, Bornemann S, and Un S (2009) pH-Dependent structures of the manganese binding Sites in oxalate decarboxylase as revealed by high-field electron paramagnetic resonance. J. Phys. Chem. B 113, 9016–9025. [PubMed: 19505123]

(25). Campomanes P, Kellett WF, Easthon LM, Ozarowski A, Allen KN, Angerhofer A, Rothlisberger U, and Richards NGJ (2014) Assigning the EPR fine structure parameters of the Mn(II) centers in Bacillus subtilis oxalate decarboxylase by site-directed mutagenesis and DFT/MM calculations. J. Am. Chem. Soc 136, 2313–2323. [PubMed: 24444454]

(26). Angerhofer A, Moomaw EW, García-Rubio I, Ozarowski A, Krzystek J, Weber RT, and Richards NGJ (2007) Multi-frequency EPR studies on the Mn(II) centers of oxalate decarboxylase. J. Phys. Chem. B 111, 5043–5046. [PubMed: 17444678]

(27). Chang CH, Svedru0žić D, Ozarowski A, Walker L, Yeagle G, Britt RD, Angerhofer A, and Richards NGJ (2004) EPR spectroscopic characterization of the manganese center and a free radical in the oxalate decarboxylase reaction - Identification of a tyrosyl radical during turnover. J. Biol. Chem 279, 52840–52849. [PubMed: 15475346]

(28). Moral MEG, Tu CK, Richards NGJ, and Silverman DN (2011) Membrane inlet for mass spectrometric measurement of catalysis by enzymatic decarboxylases. Anal. Biochem 418, 73–77. [PubMed: 21782782]

(29). Moral MEG, Tu CK, Imaram W, Angerhofer A, Silverman DN, and Richards NGJ (2011) Nitric oxide reversibly inhibits *Bacillus subtilis* oxalate decarboxylase. Chem. Commun 47, 3111–3113.

(30). Cleland WW (1979) Statistical analysis of enzyme data. Methods Enzymol. 63, 103–138. [PubMed: 502857]

(31). Stoll S, and Schweiger A (2006) EasySpin, a comprehensive software package for spectral simulation and analysis in EPR. J. Magn. Reson 178, 42–55. [PubMed: 16188474]

(32). Duboc C, Ganyushin D, Sivalingam K, Collomb MN, and Neese F (2010) Systematic theoretical study of the zero-field splitting in coordination complexes of Mn(III). Density functional theory versus multi-reference wave function approaches. J. Phys. Chem. A 114, 10750–10758. [PubMed: 20828179]

(33). Campbell KA, Force DA, Nixon PJ, Dole F, Diner BA, and Britt RD (2000) Dual-mode EPR detects the initial intermediate in photo-assembly of the photosystem II Mn cluster: The influence of amino acid residue 170 of the D1 polypeptide on Mn coordination. J. Am. Chem. Soc 122, 3754–3761.

(34). Emiliani E, and Riera B (1968) Enzymatic oxalate decarboxylation in *Aspergillus niger*. 2. Hydrogen peroxide formation and other characteristics of oxalate decarboxylase. Biochim. Biophys. Acta 167, 414–421. [PubMed: 5729956]

(35). Shook RL, Gunderson WA, Greaves J, Ziller JW, Hendrich MP, and Borovik AS (2008) A monomeric Mn(III)-peroxo complex derived directly from dioxygen. J. Am. Chem. Soc 130, 8888–8889. [PubMed: 18570414]

(36). Emerson JP, Kovaleva EG, Farquhar ER, Lipscomb JD, and Que L Jr. (2008) Swapping metals in Fe- and Mn-dependent dioxygenases: Evidence for oxygen activation without a change in metal redox state. Proc. Natl. Acad. Sci. U. S. A 105, 7347–7352. [PubMed: 18492808]

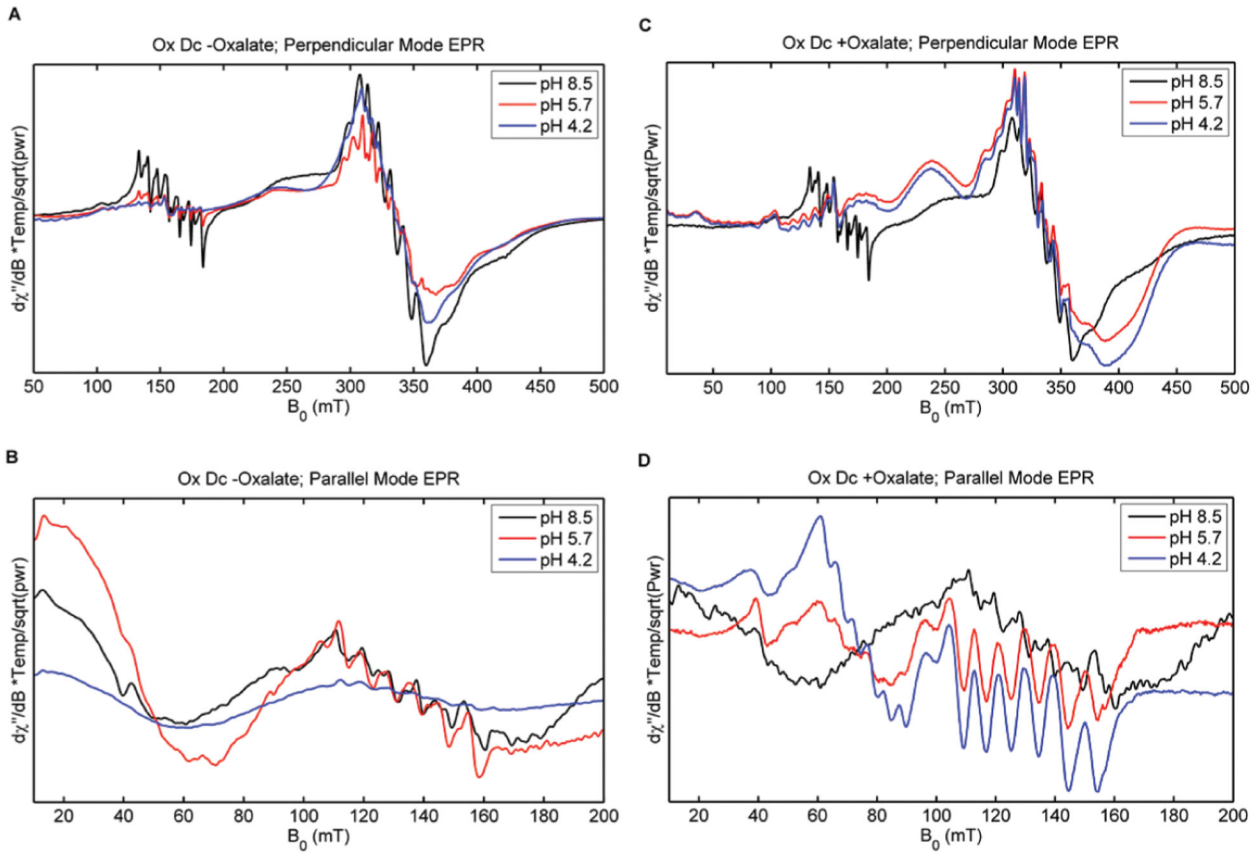

Figure 1.

(A) Perpendicular mode and (B) parallel mode EPR spectra of wt OxDC in the absence of oxalate at pH 8.5 (black), pH 5.7 (red), and pH 4.2 (blue). (C) Perpendicular mode and (D) parallel mode EPR spectra of wt OxDC in the presence of 100 mM oxalate at pH 8.5 (black), pH 5.7 (red), and pH 4.2 (blue). Perpendicular mode EPR spectra were recorded at a 9.37 GHz microwave frequency, a 0.5 mW power, and a 5 G modulation amplitude, at 10 K. Parallel mode EPR spectra were recorded at a 9.40 GHz microwave frequency, a 10 mW power, and an 8 G modulation amplitude, at 5.5 K.

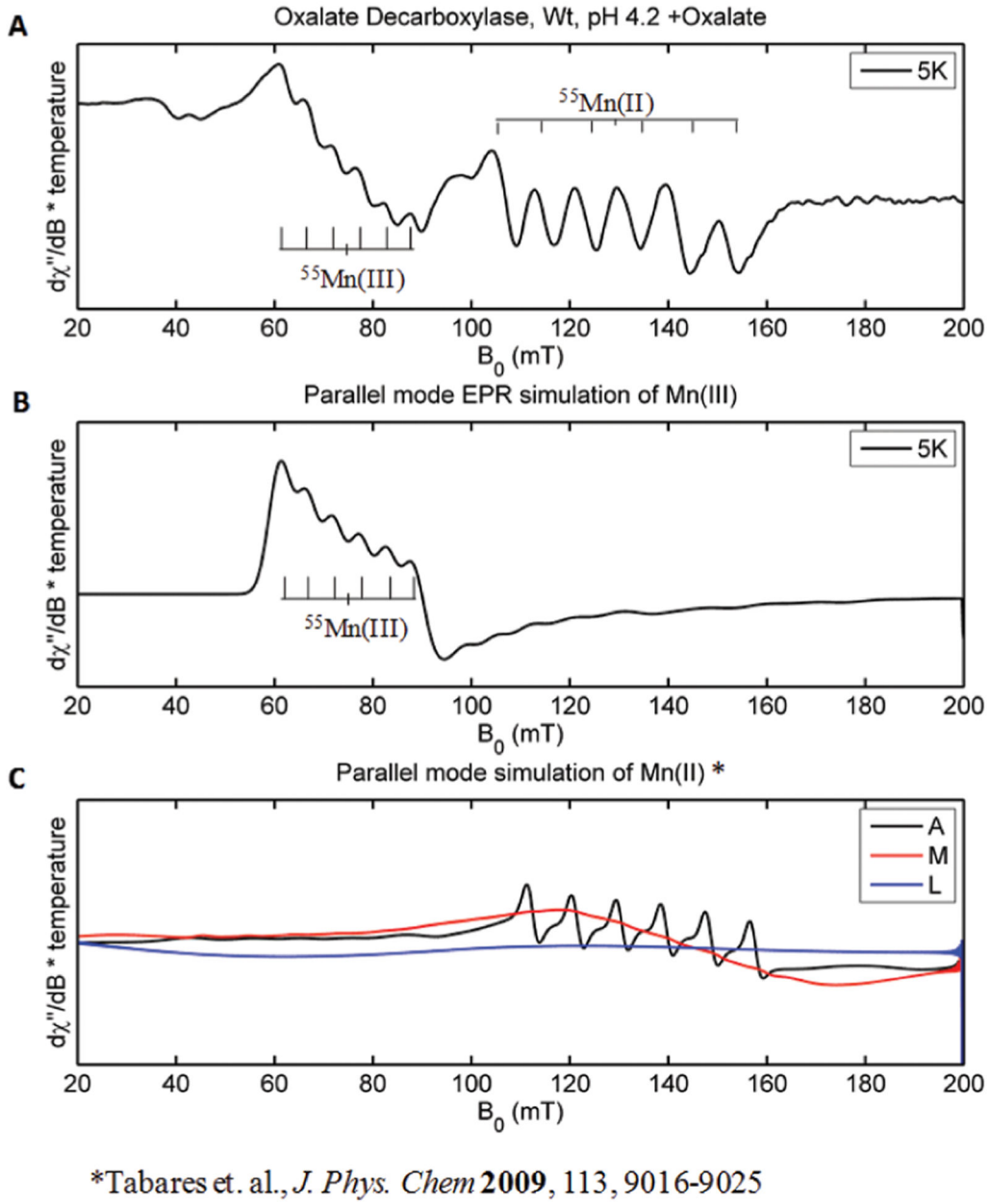

Figure 2.

Parallel mode simulations of Mn(III) in OxDC in the presence of 100 mM oxalate. (A) Spectrum of wt OxDC in the presence of oxalate at pH 4.2. “Goal Posts” indicate the Mn(II) and Mn(III) species present, distinguished by a ^{55} Mn hyperfine splitting of 253 MHz for Mn(II) and 165 MHz for Mn(III). The spectrum was recorded at 5.5 K, a 9.40 GHz microwave frequency, a 10 mW power, and an 8 G modulation amplitude. (B) Spectral simulation of the spectrum shown above with Mn(III) species indicated. Simulation parameters: $g = 2.0$, A (^{55}Mn) = 150 MHz, $D = -120$ GHz, and $|E| = 13.2$ GHz. (C) Perpendicular mode (A) and parallel mode (B) EPR spectra of wt OxDC in the absence of oxalate at pH 8.5 (black), pH 5.7 (red), and pH 4.2 (blue). Simulations of relevant Mn(II) species present at pH 4.2. Species A represents site 1 (active site), the low-pH conformation.

Species M and L represent equilibrium species at site 2 (auxiliary site) at low pH.
*Simulation parameters used were those determined by Tabares et al.[24]

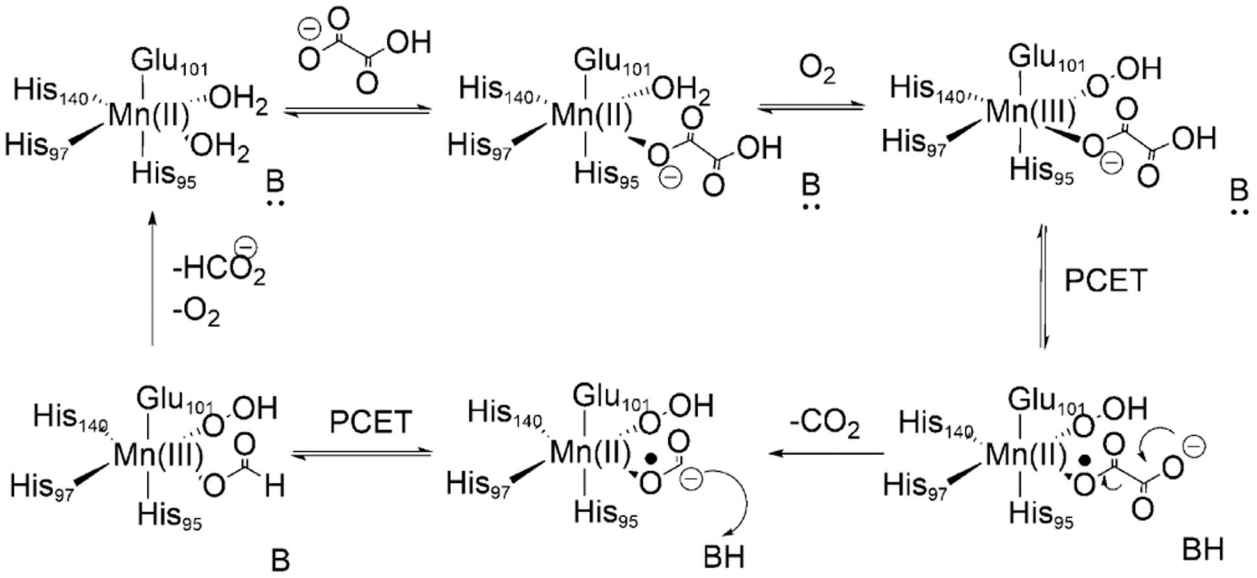

Scheme 1. Representation of a Mechanistic Proposal for OxDC-Catalyzed Conversion of Oxalate Monoanion to Formate and CO_2[8,20a]

[a]Mn(III) formation is thought to require dioxygen giving rise to superoxide anion.[14] After removal of an electron from Mn-bound substrate, in a process that may be concomitant with proton removal, decarboxylation gives a radical anion that gains a proton and an electron from Mn(II). Regeneration of Mn(II) may involve dioxygen loss or formation of a tyrosyl radical.[27]